The Plant Cell, Vol. 11, 2139–2152, November 1999, www.plantcell.org

IFL1, a Gene Regulating Interfascicular Fiber Differentiation in Arabidopsis, Encodes a Homeodomain–Leucine Zipper Protein

Ruiqin Zhong and Zheng-Hua Ye[1]

Department of Botany, University of Georgia, Athens, Georgia 30602

Arabidopsis inflorescence stems develop extraxylary fibers at specific sites in interfascicular regions. The spatial specification of interfascicular fiber differentiation is regulated by the *INTERFASCICULAR FIBERLESS1* (*IFL1*) gene because mutation of that gene abolishes the formation of normal interfascicular fibers in Arabidopsis stems. To understand further the role of IFL1 in the specification of fiber differentiation, we cloned the *IFL1* gene by using a positional cloning strategy. Sequence analysis showed that the *IFL1* gene encodes a transcription factor that has the same features as a family of homeodomain–leucine zipper (HD-ZIP) proteins found only in plants. The predicted IFL1 protein is composed of three distinct domains, including a 60–amino acid HD at the N terminus followed by a 28–amino acid ZIP motif and a 724–amino acid C-terminal region. A nuclear targeting assay showed that IFL1 is able to direct a β-glucuronidase fusion protein into the nucleus, which is consistent with IFL1's presumed function as a transcription factor. Gene expression analysis demonstrated that the *IFL1* gene is expressed in the interfascicular regions in which fibers differentiate, which is consistent with its role in the control of interfascicular fiber differentiation. Furthermore, the *IFL1* gene was shown to be expressed in the vascular regions, indicating its possible role in the regulation of vascular tissue formation. This possibility is supported by the observation that differentiation of both xylary fibers and vessel elements is altered in the vascular bundles of *ifl1* mutants. Our results provide direct evidence that an HD-ZIP protein plays a role in the spatial control of fiber differentiation.

INTRODUCTION

A plant body is composed of many different cell types. Indeed, >40 plant cell types have been defined according to their size, shape, location, wall structure, or cellular contents (Lyndon, 1990). Understanding the molecular mechanisms controlling the differentiation of different cell types is an important issue in plant biology. Recent molecular and genetic studies already have unraveled some facets of the control of differentiation of certain cell types, such as trichomes and root hairs. For example, it has been demonstrated that *GLABROUS1* (*GL1*) and *TRANSPARENT TESTA GLABRA* are required for normal trichome initiation (Larkin et al., 1997), and several other genes, including *REDUCED TRICHOME NUMBER*, *COTYLEDON TRICHOME1*, *TRIPTYCHON*, *GL2* and *GL3*, also influence trichome formation (Szymanski and Marks, 1998). Root hair initiation has been shown to be controlled by the *TRANSPARENT TESTA GLABRA* and *GL2* genes as well as by the plant hormones auxin and ethylene (Schiefelbein et al., 1997). However, our knowledge of the mechanisms controlling the formation of trichomes and root hairs is fragmentary. Much less is known about the molecular mechanisms underlying the differentiation of other plant cell types, such as tracheary elements, fibers, collenchyma, phloem sieve tubes, and companion cells.

Tracheary elements and fibers traditionally have been used as models to study cellular differentiation because they can be easily identified on the basis of their thick secondary walls. It has been shown that the plant hormone auxin is a principal inducer of the differentiation of tracheary elements and fibers (Aloni, 1987). The polar flow of auxin, which is produced in shoot apex and young leaves, induces the differentiation of tracheary elements and fibers along its paths. In addition to auxin, cytokinin also has been shown to be important for tracheary element formation (Fukuda, 1996), and cytokinin together with gibberellins are required for fiber differentiation (Aloni, 1979, 1982). Recently, the *MONOPTEROS* gene, which is important for the normal alignment of tracheary elements, has been shown to encode a transcription factor that contains a DNA binding domain able to bind to the control elements of auxin-inducible promoters (Hardtke and Berleth, 1998). The identification of MONOPTEROS as an auxin response factor provides molecular evidence for the role of auxin in vascular strand formation.

[1] To whom correspondence should be addressed. E-mail ye@dogwood.botany.uga.edu; fax 706-542-1805.

However, little is known about the molecular mechanisms controlling the spatial distribution of auxin flow paths, which most likely determines the spatial differentiation of tracheary elements and fibers. Similarly, little is known about the molecular mechanisms controlling hormonal signal transduction that induces the differentiation of tracheary elements and fibers.

In Arabidopsis inflorescence stems, the majority of fibers are present in the interfascicular regions. The interfascicular fibers are located next to the endodermis and are positioned parallel to the phloem. To dissect the mechanisms controlling fiber differentiation, we have screened for Arabidopsis mutants defective in fiber differentiation. One mutant, *interfascicular fiberless1* (*ifl1*), has been found to completely disrupt normal interfascicular fiber formation in the inflorescence stems (Zhong et al., 1997). *ifl1* stems have normal layers of cells present in the interfascicular regions, indicating that the *IFL1* gene is not involved in the control of cell division in this region but rather is involved in the initiation of fiber differentiation. It appears that the *IFL1* gene is not a general regulator for all fiber differentiation, because fibers still are formed at other locations in *ifl1* stems. In particular, in *ifl1* stems, some cells are sclerified in certain regions, whereas in the wild type, this normally does not occur (Zhong et al., 1997). This suggests that the *IFL1* gene confers spatial control of fiber differentiation in Arabidopsis inflorescence stems. Isolation of the *IFL1* gene is necessary to further our understanding of the molecular mechanisms underlying fiber differentiation.

It has been shown that in animals, the spatial control of cell differentiation and pattern formation could be regulated by homeobox genes (Graba et al., 1997). The homeobox, a 180-bp DNA element, was first found in genes that control morphogenesis of the fruit fly. The homeodomain (HD), a 60–amino acid sequence encoded by the homeobox, is a sequence-specific DNA binding domain. The HD is highly conserved among animal, fungal, and plant HD proteins. Structural analysis of the HD of the *Antennapedia* gene product has shown that the HD forms a helix-turn-helix structure, which is involved in binding specific DNA sequences (Qian et al., 1989; Gehring et al., 1990). Studies of animal homeobox genes have demonstrated that they are master control genes that are involved in pattern formation and specification of the body plan (Affolter et al., 1990; Graba et al., 1997).

Since the initial isolation of the maize *knotted1* (*kn1*) gene, which encodes an HD protein (Vollbrecht et al., 1991), many homeobox genes have been isolated from diverse plant species. Studies of plant homeobox genes have indicated that they also play master regulatory roles in plant growth and development. According to sequence similarities and organizations of conserved protein motifs, plant HD proteins generally are grouped into five families (Lu et al., 1996). The HD-KN1 family is the best characterized HD protein family, and mutational studies have indicated roles for some of the corresponding genes, such as *kn1* and *SHOOTMERISTEMLESS* (*STM*), in maintaining indeterminate cell fate (Kerstetter and Hake, 1997). The plant HD–finger (PHD) family is named for a conserved cysteine-rich region termed the HD finger (Schindler et al., 1993). No mutants in this family have been reported. In the HD-BELL1 (BEL1) family, BEL1 is shown to be required for integument development (Reiser et al., 1995). GL2 in the HD-GL2 family is involved in the formation of trichomes and root hairs (Rerie et al., 1994; Masucci et al., 1996). It is the only plant HD protein known to be important for differentiation of specific cell types.

The HD–leucine zipper (HD-ZIP) family is characterized by an HD followed by a ZIP motif. This feature is found only in plant HD proteins (Ruberti et al., 1991; Schena and Davis, 1992, 1994; Sessa et al., 1998). The ZIP motif was shown to be involved in formation of protein dimers (Sessa et al., 1993). Results from overexpression and antisense expression analyses suggest that some members of the HD-ZIP family function as developmental regulators (Schena et al., 1993; Aoyama et al., 1995; Meijer et al., 1997); however, the precise roles of the HD-ZIP family in plant growth and development still are not known.

In this study, we report the positional cloning of and expression studies with the *IFL1* gene, which regulates the interfascicular fiber differentiation in Arabidopsis inflorescence stems. Sequence analysis indicates that IFL1 has the same domain organizations as other members of the HD-ZIP family. This finding provides direct evidence that an HD-ZIP protein functions in the spatial control of the differentiation of a specific cell type—interfasicular fibers. The relationship among the *IFL1* gene, auxin polar flow, and the spatial control of fiber differentiation is discussed.

RESULTS

Fine Mapping of the *ifl1* Locus

The *ifl1* mutant was isolated from ethyl methanesulfonate (EMS)–mutagenized populations of Arabidopsis (Zhong et al., 1997). Thus, the positional cloning approach was used to fine map the *ifl1* locus and isolate the *IFL1* gene. Previous mapping results showed that the *ifl1* locus is located between markers 7H9L and 17C2 on chromosome 5 (Zhong et al., 1997). Markers 7H9L and 17C2 are located in the yeast artificial chromosome (YAC) clones yUP7H9 and yUP17C2, respectively. According to YAC contig 29 of chromosome 5, the YAC clone yUP7H9 overlaps yUP17C2 (AtDB Web site: http://nasc.nott.ac.uk/JIC-contigs/Chr5_YACcontigs.html; Schmidt et al., 1997). To test whether the 17C2 marker is located within the yUP7H9 YAC clone, we used yeast genomic DNA containing yUP7H9 DNA as the template in polymerase chain reactions (PCRs) with primers derived from the 17C2 marker. The 17C2 primers specifically amplified a fragment with the expected length of 1.4 kb, indicat-

ing that the 17C2 marker is located in yUP7H9. This suggests that the *ifl1* locus, which was mapped to a region between markers 7H9L and 17C2, is located in the YAC clone yUP7H9 (Figure 1A).

To locate the *ifl1* locus within bacterial artificial chromosome (BAC) clones, we screened the P1 library (Liu et al., 1995) by using PCR with primers 7H9L and 17C2. When the BAC clone MIUP24 was used as a template, both primers 7H9L and 17C2 amplified fragments with expected lengths of 1.9 and 1.4 kb, respectively. This indicated that the *ifl1* locus was within the BAC clone MIUP24 (Figure 1A).

Because two plants used for mapping had crossovers between the *ifl1* locus and the 7H9L marker and two for mapping had crossovers between the *ifl1* locus and the 17C2 marker (Zhong et al., 1997; Figure 1B), we decided to develop new markers to further fine map the *ifl1* locus. MIUP24 BAC DNA was isolated and digested with restriction enzymes BamHI, EcoRI, or EcoRV. The digested DNA fragments were ligated into the pBluescript KS+ vector, and the ends of some of the DNA inserts were sequenced. According to the end sequences, new primers were designed for developing the codominant cleaved amplified polymorphic sequence (CAPS) markers mup24B3, mup24RI-6A, mup24RV-7B, mup24B4, and mup24B2 (Figure 1B).

Further mapping with these new markers showed that one plant possessed a crossover between the *ifl1* locus and the mup24RI-6A marker when the mapping plants with crossovers between the *ifl1* locus and the 7H9L marker were used. Similarly, there was one plant with a crossover between the *ifl1* locus and the mup24B2 marker when the mapping plants with crossovers between the *ifl1* locus and the 17C2 marker were used. This placed the *ifl1* locus within a region between the mup24RI-6A and mup24B2 markers (Figure 1B).

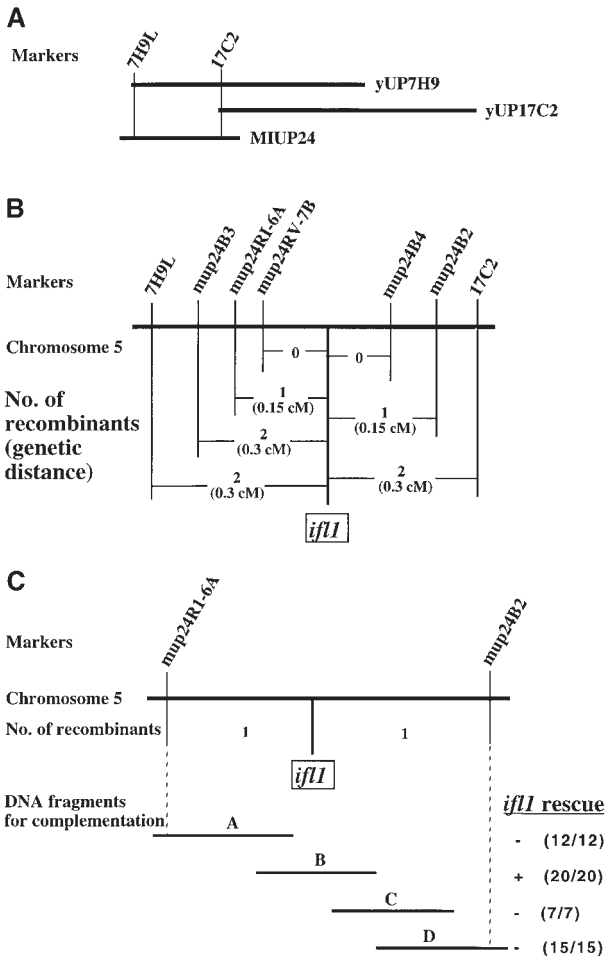

Figure 1. Positional Cloning of the *IFL1* Gene.

(A) Diagram of the YAC (yUP7H9 and yUP17C2) and BAC (MIUP24) clones spanning the region in which the markers 7H9L and 17C2 are located. The *ifl1* locus previously was mapped to a region between 7H9L and 17C2.

(B) Fine mapping of the *ifl1* locus. The BAC clone MIUP24 was used to develop CAPS markers for fine mapping the *ifl1* locus. The *ifl1* locus was narrowed to a 0.3-centimorgan (cM) region covered by markers mup24RI-6A and mup24B2.

(C) DNA fragments used for complementation of the *ifl1* mutation. Four overlapping DNA fragments covering the *IFL1* locus were introduced into the *ifl1* mutant. It was found that the DNA fragment B completely rescued the *ifl1* mutation. (−) indicates no rescue; (+) indicates a complete rescue of the *ifl1* mutation. The numbers in the parentheses indicate the number of plants with the indicated phenotype out of the total number of transgenic plants examined.

Complementation of the *ifl1* Mutant

To clone the *IFL1* gene, we constructed a plasmid contig spanning the region between the mup24RI-6A and mup24B2 markers and then examined their ability to complement the *ifl1* mutation. Partially digested DNA fragments of MIUP24 BAC DNA with lengths of ~10 kb were ligated into the pBluescript KS+ vector to create an MIUP24 plasmid library. The library was screened by using PCR with the mup24RI-6A and mup24B2 marker primers, and positive clones were selected for sequencing of fragment ends. New primers were designed according to the end sequences of the fragments and used to further screen the library by using PCR. It was found that four overlapping fragments (fragments A, B, C, and D) with lengths of ~10 to 14 kb covered the region between the markers mup24RI-6A and mup24B2 (Figure 1C). These four fragments were cloned into the binary vector pBI101. Agrobacteria containing these constructs were used to transform the *ifl1* plants.

Transgenic *ifl1* plants were examined for restoration of wild-type phenotypes. The *ifl1* mutant did not form fibers at the normal position of interfascicular regions, and it exhibited pleiotropic phenotypes, including long and pendent stems and reduced numbers of cauline leaves and branches (Zhong et al., 1997; Figures 2A and 2B). It was found that

whereas *ifl1* plants transformed with DNA fragment A, C, or D still had *ifl1* phenotypes, *ifl1* plants transformed with DNA fragment B showed a phenotype indistinguishable from that of the wild type (Figure 2). In the *ifl1* plants transformed with DNA fragment B, interfascicular fibers were formed at the normal, wild-type positions (Figure 2C). In addition, the inflorescence stems stood erect and had normal numbers of cauline leaves and branches (Figure 2D). These results conclusively demonstrate that DNA fragment B can completely rescue the *ifl1* mutant, and therefore it contains the *IFL1* gene.

Identification of the *IFL1* Gene

To locate the *IFL1* gene in DNA fragment B, we sequenced DNA fragment B by the primer walking strategy. Putative genes located in DNA fragment B were searched by the

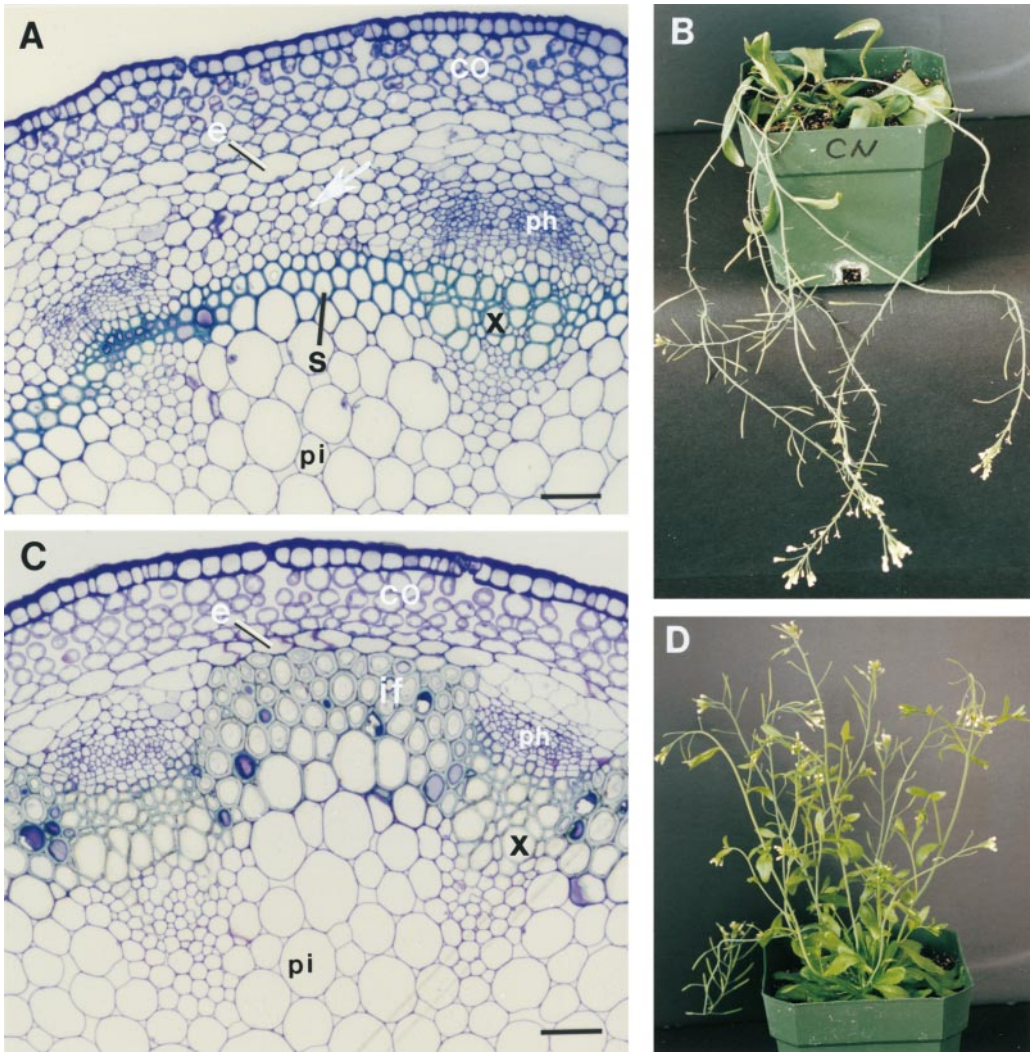

Figure 2. The 10-kb DNA Fragment B Rescues the Phenotypes of the *ifl1* Mutant.

(A) A cross-section of an *ifl1* stem showing the absence of normal interfascicular fibers. The arrow indicates the position at which interfascicular fibers are normally formed.
(B) An *ifl1* mutant plant showing the pendent stem phenotype.
(C) A cross-section of a stem from an *ifl1* mutant plant transformed with DNA fragment B showing the presence of normal interfascicular fibers.
(D) An *ifl1* mutant plant transformed with the DNA fragment B showing a wild-type phenotype.
co, cortex; e, endodermis; if, interfascicular fiber; ph, phloem; pi, pith; s, sclerenchyma; x, xylem. Bars in **(A)** and **(C)** = 5 μm.

Baylor College of Medicine (BCM) gene finder program (Web site: http://dot.imgen. bcm.tmc.edu). The program identified only one putative gene within the 10-kb DNA fragment B. The putative gene covered the 4193 bp of the predicted transcribed sequence (Figure 3A). To test whether this putative gene was the *IFL1* gene, we PCR-amplified the putative gene from the *ifl1* and *ifl1-2* mutants and then sequenced it. (The *ifl1-2* mutant, which showed phenotypes similar to those of the *ifl1* mutant, was isolated during our mutant screening. Complementation analysis showed that *ifl1-2* was allelic to *ifl1*.) Comparison of the DNA sequence of the 4193-bp putative gene from the wild type and the mutants showed that point mutations occurred in both *ifl* mutants. In the *ifl1* mutant, the nucleotide G at position 2086 within the transcribed sequence was changed to an A residue. This mutation created a new MseI site (TTAG in the wild type was converted into TTAA in *ifl1*; Figure 3B) in the putative gene, which could be detected by MseI digestion of a DNA fragment amplified from the *ifl1* genomic DNA (Figure 3D). In the *ifl1-2* mutant, the nucleotide C at position 635 was changed to a T residue (Figure 3A). These GC-to-AT point mutations in the *ifl* mutants are consistent with the mode of action of EMS, the mutagen that was used to generate the mutagenized population from which the *ifl* mutants were identified. These sequence analyses suggest that the gene predicted by the BCM gene finder program most likely represents the *IFL1* gene.

DNA fragment B was used as a probe to isolate the corresponding cDNA from an Arabidopsis stem cDNA library. Seven positive cDNA clones were isolated, and all of them cross-hybridized with each other. This indicated that they belonged to the same group of cDNAs. The cDNA clone with the longest insert was chosen for DNA sequencing. The cDNA sequence was shown to match the genomic sequence of the predicted gene and to contain the full-length predicted transcribed sequence. To further confirm that the predicted gene was indeed the *IFL1* gene, we fused the longest cDNA clone downstream of a 2.3-kb promoter fragment of the predicted *IFL1* gene and tested whether it was able to rescue the *ifl1* mutant phenotype. As expected, *ifl1* plants transformed with this cDNA construct showed wild-type phenotypes, including the formation of interfascicular fibers at the normal positions and the upright growth of inflorescence stems (data not shown), which were the same as the phenotypes rescued by DNA fragment B (Figure 2). These results unequivocally demonstrate that the predicted gene represents the *IFL1* gene.

Comparison of the *IFL1* cDNA and *IFL1* genomic DNA sequences identified 18 exons and 17 introns in the transcribed unit of the *IFL1* gene (Figure 3A). The point mutation (G to A) that occurred in the *ifl1* mutant disrupted the ninth intron splicing acceptor site (Figures 3A and 3B). Coincidentally, the nucleotide directly after the point mutation was a G, creating a new AG sequence that potentially could be used as a new intron splicing acceptor site. Sequencing of the *ifl1* cDNA from the *ifl1* mutant confirmed that this new

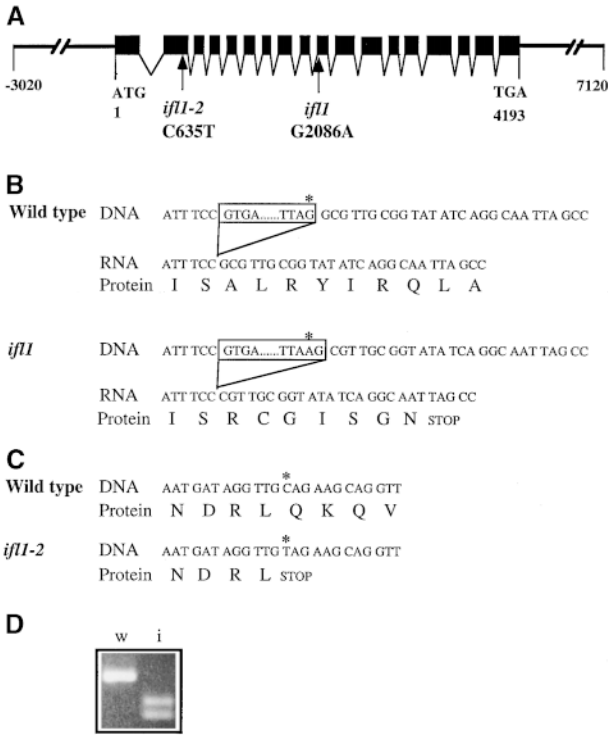

Figure 3. Structure of the *IFL1* Gene and the Nature of the Mutations in the *ifl1* Alleles.

(A) A schematic representation of the exon and intron organization of the *IFL1* gene. The *IFL1* gene is 4193 bp long, starting from the start codon (designated nucleotide 1) to the stop codon (designated nucleotide 4193). Single nucleotide mutations were found in both *ifl1* (the G at nucleotide position 2086 is changed to an A) and *ifl1-2* (the C at nucleotide position 635 is changed to a T). Black boxes denote exons. Lines between black boxes denote introns.

(B) Effect of the single nucleotide mutation in the *ifl1* mutant on the translation of the predicted protein. Shown are residues around the mutation site. The G-to-A transition at the intron splicing acceptor site resulted in aberrant splicing. This aberrant splicing leads to a coding frameshift, thus generating a premature stop codon at the eighth codon after the mutation site. The mutated nucleotides are indicated by asterisks. Boxed sequences are introns that are spliced out in the mature mRNA. Dots denote nucleotides in the intron.

(C) Effect of the single nucleotide mutation in the *ifl1-2* mutant on the translation of the predicted protein. Shown are residues around the mutation site. The C-to-T transition creates a nonsense mutation. The mutated nucleotides are indicated by asterisks.

(D) Creation of a new MseI site in the mutant *ifl1* gene. A DNA fragment covering the *ifl1* mutation site was PCR-amplified from the wild type and the *ifl1* mutant genomic DNA. After digestion with MseI, DNA fragments were separated on an agarose gel containing ethidium bromide and visualized under UV light. The DNA fragment amplified from the *ifl1* mutant was cut into two pieces due to the creation of a new MseI site (TTAG is changed to TTAA) by the *ifl1* mutation (lane i), whereas the DNA fragment amplified from the wild type was not cut (lane w).

AG sequence indeed was used as the intron splicing acceptor site (Figure 3B). This led to a frameshift of the coding sequence that in turn led to creation of a premature stop codon in the *ifl1* cDNA (Figure 3B). The point mutation in the *ifl1-2* mutant occurred in the second exon of the *IFL1* gene (Figure 3A), and the mutation (C to T) created a premature stop codon (Figure 3C).

The *IFL1* cDNA is 3159 bp long, which is consistent with the length of the 3.3-kb mRNA detected with the *IFL1* cDNA probe on the RNA gel blot. The longest open reading frame encodes a polypeptide of 840 amino acids (Figure 4) with a predicted molecular mass of 92,178 D. In addition, the *IFL1* cDNA has a long 5′ untranslated region with >500 nucleotides beyond the translation start codon.

The *IFL1* Gene Encodes an HD-ZIP Protein

Sequence comparison of the deduced amino acid sequence of IFL1 with the GenBank database showed that IFL1 exhibits high similarity to a group of HD-ZIP transcription factors. The N-terminal amino acid sequence (residues 24 to 116) of IFL1 exhibited 84 to 88% identity to the HD-ZIP regions of group III HD-ZIP proteins, Athb8, Athb9, and Athb14 (Figure 5A). It shares 20 to 35% identity with the HD-ZIP regions of other HD-ZIP proteins. The HD (residues 19 to 78) of IFL1 also shares 35 to 40% identity with the HDs of many plant and animal HD proteins. It was found that the highly conserved amino acids (Figure 5A) observed in the HDs of plant and animal HD proteins were retained in the HD of IFL1. Like

```
MAVANHRERSSDSMNRHLDSSGKYVRYTAEQVEA 34
LERVYAECPKPSSLRRQQLIRECSILANIEPKQI 68
KVWFQNRRCRDKQRKEASRLQSVNRKLSAMNKLL 102
MEENDRLQKQVSQLVCENGYMKQQLTTVVNDPSC 136
ESVVTTPQHSLRDANSPAGLLSIAEETLAEFLSK 170
ATGTAVDWVQMPGMKPGPDSVGIFAISQRCNGVA 204
ARACGLVSLEPMKIAEILKDRPSWFRDCRSLEVF 238
TMFPAGNGGTIELVYMQTYAPTTLAPARDFWTLR 272
YTTSLDNGSFVVCERSLSGSGAGPNAASASQFVR 306
AEMLSSGYLIRPCDGGGSIIHIVDHLNLEAWSVP 340
DVLRPLYESSKVVAQKMTISALRYIRQLAQESNG 374
EVVYGLGRQPAVLRTFSQRLSRGFNDAVNGFGDD 408
GWSTMHCDGAEDIIVAINSTKHLNNISNSLSFLG 442
GVLCAKASMLLQNVPPAVLIRFLREHRSEWADFN 476
VDAYSAATLKAGSFAYPGMRPTRFTGSQIIMPLG 510
HTIEHEEMLEVVRLEGHSLAQEDAFMSRDVHLLQ 544
ICTGIDENAVGACSELIFAPINEMFPDDAPLVPS 578
GFRVIPVDAKTGDVQDLLTANHRTLDLTSSLEVG 612
PSPENASGNSFSSSSSRCILTIAFQFPFENNLQE 646
NVAGMACQYVRSVISSVQRVAMAISPSGISPSLG 680
SKLSPGSPEAVTLAQWISQSYSHHLGSELLTIDS 714
LGSDDSVLKLLWDHQDAILCCSLKPQPVFMFANQ 748
AGLDMLETTLVALQDITLEKIFDESGRKAICSDF 782
AKLMQQGFACLPSGICVSTMGRHVSYEQAVAWKV 816
FAASEENNNNLHCLAFSFVNWSFV            840
```

Figure 4. Amino Acid Sequence Deduced from the *IFL1* cDNA.

The GenBank accession number for the *IFL1* cDNA sequence data is AF188994.

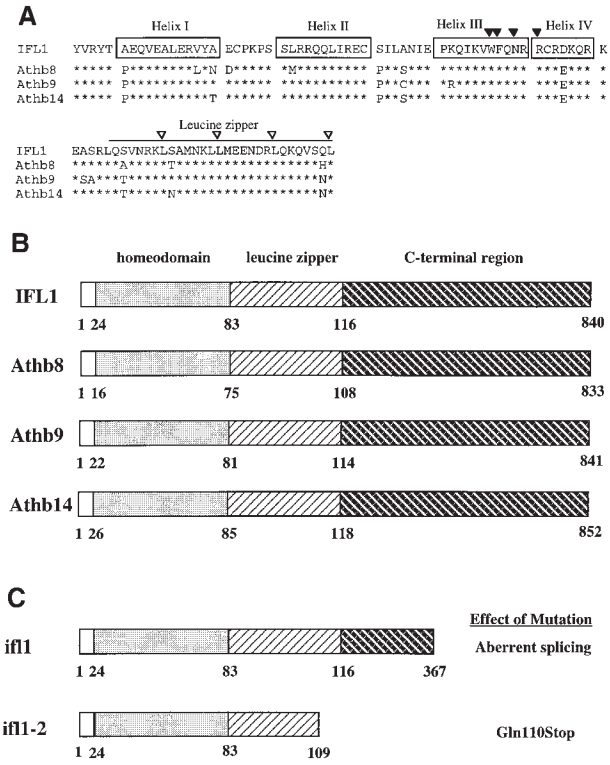

Figure 5. Comparison of the Domains of the IFL1 Protein and the Other Group III HD-ZIP Proteins.

(A) Alignment of the amino acid sequences in the HD and ZIP motifs. Amino acid residues identical to the ones in IFL1 are marked with asterisks. Amino acid sequences involved in the formation of the helix-turn-helix structure in the HD of IFL1 are boxed. The invariant amino acid residues in the HD are marked with solid triangles. The ZIP motif is labeled, and the leucine residues that occur at every seventh position in the ZIP motif are marked with open triangles.

(B) Diagrams of the domains of IFL1 and the other group III HD-ZIP proteins. All of these proteins are similar in length, and they have the same domain organization. The names of individual domains are indicated above the IFL1 diagram. The numbers below each diagram indicate the amino acid positions of each domain.

(C) Diagrams of the domains of the truncated ifl mutant proteins. The deduced ifl1 mutant protein contains intact HD and ZIP motifs and a partial (244 amino acid residues) C-terminal region. The deduced ifl1-2 mutant protein contains an intact HD and most of the ZIP motif (one ZIP repeat is missing). The entire C-terminal region is missing in the ifl1-2 mutant protein. Gln110Stop denotes the glutamine at residue 110 in the wild-type protein that was changed to a stop codon in the ifl1-2 mutant protein.

other plant HD-ZIP proteins, the HD of IFL1 was followed by a ZIP motif that spans residues 83 to 116 (Figures 5A and 5B). It is known that ZIP motifs are composed of a stretch of amino acids with a leucine residue in every seventh position, and they can interact with each other to form dimers (Lewin, 1990). The ZIP motif in IFL1 has this typical pattern: all four of the seven–amino acid repeats has a leucine residue at every seventh position. Comparison of the *IFL1* cDNA and *IFL1* genomic DNA sequences showed that the HD is located in the first exon and the ZIP motif in the second exon of the *IFL1* gene.

In addition to the HD-ZIP region, IFL1 has a long C-terminal region with 724 amino acid residues (Figure 5B). The C-terminal region of IFL1 shares ~60 to 65% sequence identity with the C-terminal regions of the group III HD-ZIP proteins Athb8, Athb9, and Athb14 (Sessa et al., 1998). The C-terminal regions of all of these proteins are similar in length (Figure 5B), and sequence similarity was observed throughout the region. The IFL1 C-terminal region did not show sequence similarity to any other proteins in the database. These results strongly suggest that the *IFL1* gene encodes a group III HD-ZIP protein.

Analysis of the deduced amino acid sequence from the *ifl1* mutant cDNAs showed that in the *ifl1* mutant, a stop codon was created at residue 368 due to a frameshift that resulted from aberrant splicing. The encoded ifl1 mutant protein retained the HD, the ZIP motif, and 244 residues of the C-terminal region (Figure 5C). In the *ifl1-2* mutant, the glutamine residue at amino acid position 110 was changed to a stop codon due to a point mutation. This resulted in the loss of one ZIP repeat and the entire C-terminal region in the ifl1-2 mutant protein (Figure 5C).

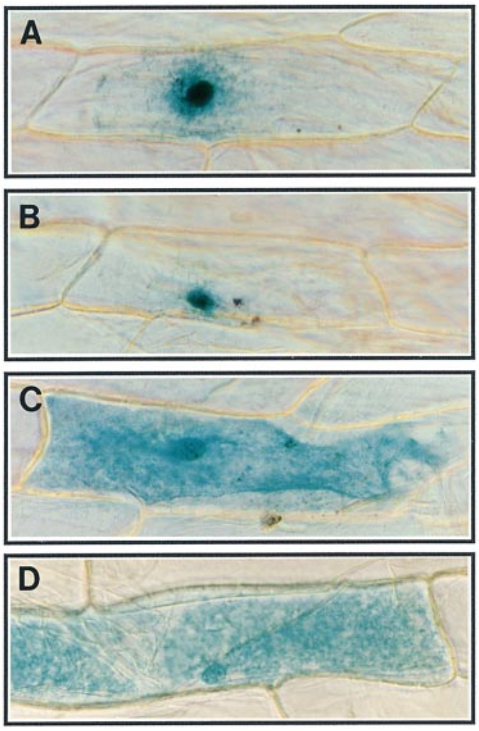

Figure 6. Nuclear Localization of the IFL1–GUS Fusion Proteins in Onion Epidermal Cells.

Full-length IFL1 or different domains of IFL1 were fused in-frame to the N terminus of GUS in the expression vector pBI221. Plasmid DNA was delivered into onion cells by using a particle bombardment procedure. After 16 hr of incubation, cells were stained for GUS activity (shown as blue) and observed under a differential interference contrast microscope.

(A) The full-length IFL1–GUS fusion protein showing GUS staining only in the nucleus.

(B) The HDZ–GUS fusion protein showing GUS staining only in the nucleus.

(C) The C-terminal region–GUS fusion protein showing GUS staining in the cytoplasm.

(D) The control GUS protein showing staining in the cytoplasm.

Nuclear Localization of IFL1

Because the *IFL1* gene encodes a putative HD transcription factor, we investigated the ability of IFL1 to direct nuclear localization. cDNAs encoding IFL1 or its domains were fused to the β-glucuronidase (*GUS*) reporter gene, and the localization of the fusion proteins was tested by transient expression of the fusion proteins in onion epidermal cells. When the full-length *IFL1* cDNA was fused to the *GUS* reporter gene, the fusion protein was directed to the nucleus because the GUS staining was only present in the nucleus (Figure 6A). When the DNA sequence containing both the HD and the ZIP motif (HDZ) was fused to the *GUS* reporter gene, the HDZ–GUS fusion protein also was located in the nucleus (Figure 6B). However, strong GUS staining in the cytosol was seen when the fusion protein comprising the C-terminal region of IFL1 and the *GUS* reporter gene was expressed (Figure 6C). The *GUS* reporter gene alone was localized to the cytosol (Figure 6D), confirming that the nuclear localization of the GUS fusion protein conferred by the full-length IFL1 or the HDZ region of IFL1 was specific. The results were consistent with the presence of a putative nuclear localization signal within the HDZ region of IFL1 (amino acid residues 66 to 94).

Expression Pattern of the *IFL1* Gene

It has been shown that mutation of the *IFL1* gene results in disruption of normal interfascicular fiber differentiation in the inflorescence stems (Zhong et al., 1997). To examine the correlations between the phenotypes of the *ifl1* mutants and the *IFL1* expression pattern, we studied the expression of

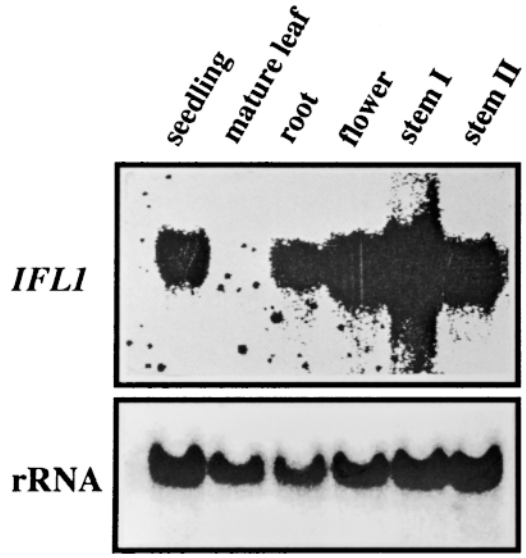

Figure 7. RNA Gel Blot Analysis of *IFL1* Gene Expression in Arabidopsis Organs.

Total RNA was isolated from different organs of Arabidopsis plants and used for RNA gel blot analysis. The gene-specific probe containing the 5′ untranslated region of the *IFL1* gene was used to probe the blot. Equal loading of RNA in each lane was confirmed by hybridizing the blot with the 18S rDNA probe. The seedlings were 3 weeks old. Mature leaves, roots, and flowers were from 8-week-old plants. Stems I and II were from 4- and 8-week-old plants, respectively.

the *IFL1* gene in both organs and tissues. RNA gel blot analysis showed that the *IFL1* gene was expressed in all organs, except for mature leaves, in which *IFL1* mRNA could not be detected (Figure 7). Expression of the *IFL1* gene in different tissues also was examined by expressing the *GUS* reporter gene under the control of the 2.3-kb *IFL1* promoter. Because expressing the *IFL1* cDNA under the control of the 2.3-kb *IFL1* promoter rescued the phenotypes of the *ifl1* mutants (see above), the *GUS* expression pattern should reflect the expression pattern of the endogenous *IFL1* gene.

Analysis of GUS activity in the inflorescence stems showed that GUS staining was evident in the interfascicular regions in which fibers were normally formed (Figures 8A and 8B). GUS activity also was shown to be present in the vascular bundles (Figures 8A and 8B). Association of the *GUS* expression with vascular strands was observed in young roots (Figure 8C), young leaves (Figure 8D), and the cotyledon (Figure 8E). No staining was evident in mature leaves (data not shown), which was consistent with the RNA gel blot analysis. These results indicate that the *IFL1* gene is preferentially expressed in the interfascicular regions as well as in vascular bundles in Arabidopsis stems. The GUS staining pattern was confirmed by in situ mRNA localization showing the presence of the *IFL1* mRNA in both interfascicular and fascicular regions (Figure 8F). The control section hybridized with the sense *IFL1* RNA probe did not show any signal (Figure 8G).

Effects of the *ifl1* Mutation on Vascular Differentiation

The finding that the *IFL1* gene was expressed in vascular bundles prompted us to examine whether any alteration in vascular differentiation was evident in the *ifl1* mutant. A close examination of the vascular anatomy in both *ifl1* and *ifl1-2* mutants showed a dramatic reduction in the numbers of vascular cells in the bundles. In the upper parts of the stems of 7-week-old plants, no major differences were observed in the vascular anatomy of wild-type (Figure 9A), *ifl1* (Figure 9B), and *ifl1-2* (Figure 9C) plants. In the middle parts of the stems, the vascular bundles in both the wild type (Figure 9D) and *ifl1* (Figure 9E) plants developed secondary xylem with the presence of vessel elements and xylary fibers. However, no secondary xylem differentiation was evident in the vascular bundles of the *ifl1-2* mutant, and only vessel elements were present in the bundles (Figure 9F).

A marked difference was detected in the vascular bundles of the basal parts of the stems of wild-type and mutant plants. The vascular bundles in the wild type underwent more secondary xylem differentiation with formation of a large proportion of xylary fibers (Figure 9G), whereas the vascular bundles in both the *ifl1* (Figure 9H) and *ifl1-2* (Figure 9I) mutants contained only a few vessel elements, apparently due to lack of secondary xylem differentiation. It was obvious that the *ifl1-2* mutant displayed a more pronounced effect on xylem differentiation than did the *ifl1* mutant. The number of phloem cells also appeared to be reduced, probably as a consequence of a lack of secondary vascular differentiation. Taken together, these results indicate that the *ifl* mutation resulted in a loss of xylary fiber differentiation and a reduction in vessel element formation.

DISCUSSION

IFL1 Is a Member of HD-ZIP Protein Family

A number of HD-ZIP genes have been isolated in Arabidopsis by screening cDNA and genomic DNA libraries with the homeobox consensus sequence (Ruberti et al., 1991; Schena and Davis, 1992, 1994). These genes generally are divided into four groups according to the degree of sequence identity (Lu et al., 1996). IFL1 shares high sequence identity to and has the same organization of domains with members in the group III HD-ZIP proteins (Figure 5), indicating that IFL1 is a new member of this group. The three other group III members, Athb8, Athb9, and Athb14, have been characterized in Arabidopsis (Sessa et al., 1998), in which they appear to be expressed in all organs. The *Athb8* gene

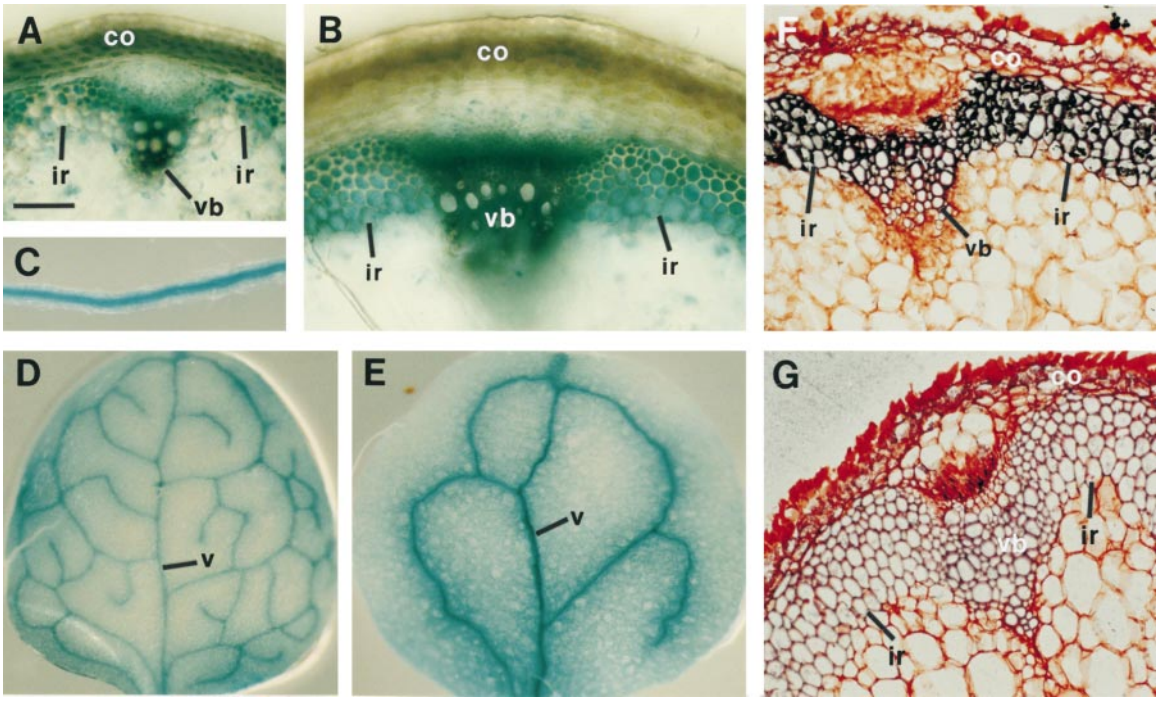

Figure 8. Expression Pattern of the *IFL1* Gene Revealed by Using the *IFL1* Promoter Activity Assay and in Situ mRNA Localization.

The 2.3-kb *IFL1* gene promoter was inserted upstream of the GUS coding sequence in the expression vector pBI121. Agrobacteria containing the expression construct were used to transform Arabidopsis plants, and transgenic plants were selected and used for GUS activity assays. GUS activity is revealed by blue staining. Signals corresponding to mRNA localization appear as black patches that result from the silver enhancement.

(A) and **(B)** Sections from the upper **(A)** and lower **(B)** parts of a stem from a 5-week-old transgenic plant. GUS staining was mainly associated with interfascicular regions and vascular bundles.

(C) to **(E)** A young root **(C)**, a young leaf **(D)**, and a cotyledon **(E)** showing GUS staining in vascular strands.

(F) In situ localization of *IFL1* mRNA showing signals in the interfasicular regions and vascular bundles in a stem section.

(G) A control section incubated with the sense *IFL1* RNA probe showing the absence of signals.

co, cortex; ir, interfascicular region; v, vein; vb, vascular bundle. Bar in **(A)** = 11 μm for **(A)**, **(B)**, **(F)**, and **(G)**.

appears to be specifically expressed in the procambial region of vascular bundles (Baima et al., 1995). The fact that mutation of the *IFL1* gene alone completely disrupts normal interfascicular fiber differentiation suggests that the *Athb8*, *Athb9*, and *Athb14* genes might have their own unique functions. It will be interesting to investigate whether these genes also play important roles in the differentiation of certain cell types.

IFL1 domain organization is similar to that of the HD-ZIP protein family, that is, the HD located at the N terminus is followed by the ZIP motif. The specific HD binding DNA sequences have been elucidated for several HD-ZIP proteins, including Athb1, Athb2, and Athb9 (Sessa et al., 1993, 1998). The ZIP motifs in Athb1, Athb2, and Athb9 have been shown to be involved in dimerization of these proteins, which is essential for DNA binding (Sessa et al., 1993). According to the pronounced sequence similarity between Athb9 and IFL1, it is reasonable to predict that IFL1 forms a dimer through the ZIP motif and that the dimerized IFL1 binds to a specific DNA sequence through the HD. It is important to identify the DNA sequence to which IFL1 binds to search for IFL1 target genes.

IFL1 possesses a long C-terminal region with 720 amino acid residues. This region of IFL1 does not show any sequence identity to any known functional domains, with the exception of the C-terminal regions of the group III HD-ZIP proteins. If, as predicted, the HD and ZIP motifs of IFL1 are involved in sequence-specific DNA binding, then the C-terminal region most likely interacts directly or indirectly with other transcription machinery to activate or suppress expression of target genes. It is interesting that the *ifl1* mutant, in which only a portion of the C-terminal region is missing, has much less effect on vascular differentiation than does the *ifl1-2* mutant, in which the entire C-terminal region is missing (Figure 9). This indicates that the 244 amino acid residues that remain in the C-terminal region of the ifl1

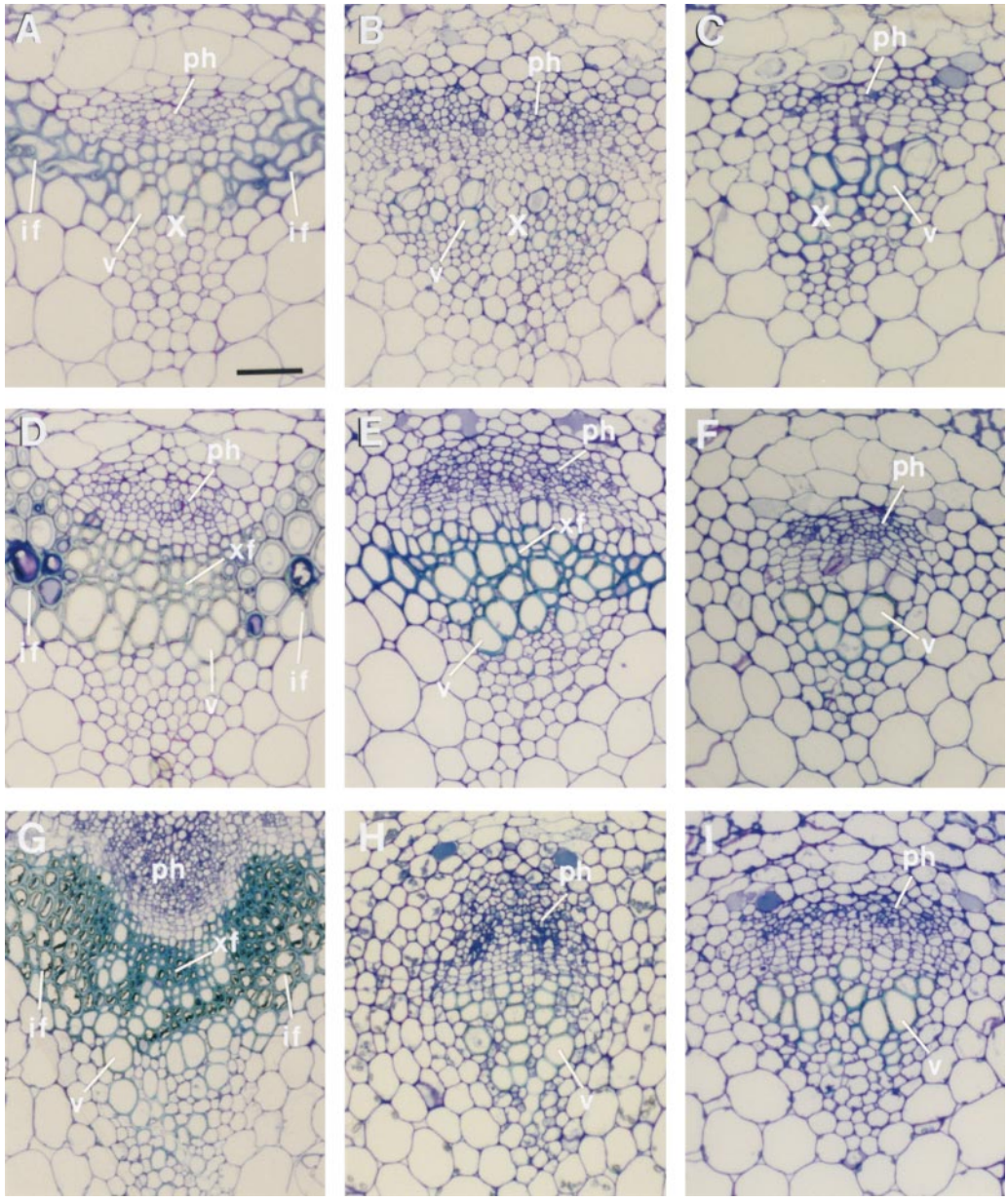

Figure 9. Effects of the *ifl* Mutations on the Vascular Differentiation in Inflorescence Stems.

Thin sections were prepared from stems of 7-week-old wild-type, *ifl1*, and *ifl1-2* plants and stained with toluidine blue to reveal anatomy.
(A) to **(C)** Sections from the top segments of the stems from the wild-type **(A)**, *ifl1* **(B)**, and *ifl1-2* **(C)** plants. No xylary fibers were evident in the vascular bundles in all of these plants.
(D) to **(F)** Sections from the middle segments of the stems from the wild type **(D)**, *ifl1* **(E)**, and *ifl1-2* **(F)** plants. Xylary fibers were evident in both the wild-type and the *ifl1* plants but not in the *ifl1-2* plants.
(G) to **(I)** Sections from the basal segments of the stems from the wild type **(G)**, *ifl1* **(H)**, and *ifl1-2* **(I)** plants. In the bottom parts of the stems, although the vascular bundles in the stems of the wild-type plants developed many xylary fibers, the vascular bundles in the stems of both *ifl1* and *ifl1-2* mutant plants were devoid of xylary fibers.
if, interfascicular fiber; ph, phloem; v, vessel element; X, xylem; xf, xylary fiber. Bar in **(A)** = 5 μm for **(A)** to **(I)**.

mutant protein (Figure 5) still may retain some activity, whereas the *ifl1-2* mutation (Figure 5) most likely acts as a null mutation. It will be interesting to further dissect the functions of the C-terminal region of IFL1 by deletion and functional expression analyses.

Role of IFL1 in the Positional Control of Fiber Differentiation

Most plant HD proteins characterized to date have been implicated in meristem maintenance and organ development (Kerstetter and Hake, 1997). IFL1 is one of a few HD proteins known to regulate cell differentiation. The only other known HD protein involved in cell differentiation is GL2, which has been shown to regulate the formation of trichomes and root hairs (Rerie et al., 1994; Masucci et al., 1996). The important question is how IFL1, an HD-ZIP protein, specifies the spatial control of interfascicular fiber differentiation.

It has been shown that both vascular strands and fibers are induced along the paths of auxin flow (Aloni, 1987). Thus, it is reasonable to predict that in Arabidopsis inflorescence stems, auxin flows through the interfascicular regions and induces the formation of interfascicular fibers along its paths. If this is the case, the sites of fiber differentiation are determined by the positional control of auxin flow paths. One obvious question remains to be answered: what role does IFL1 play in the relationship between auxin polar flow and interfascicular fiber differentiation?

There are two possibilities regarding the functions of IFL1. One possibility is that IFL1 might regulate genes involved in controlling the flow of auxin along the interfascicular regions. Mutations in IFL1 could abolish auxin flow along the interfascicular regions, thus leading to disruption of interfascicular fiber differentiation. The other possibility is that IFL1 might regulate genes involved in the transduction of hormonal signals leading to interfascicular fiber differentiation. In this case, mutations in IFL1 could abolish hormone signal transduction, thus leading to disruption of interfascicular fiber differentiation. These two possibilities can be tested experimentally. If the former possibility is true, then we would expect to see an alteration in the auxin polar transport activity in the *ifl1* mutant inflorescence stems. If the latter possibility is true, then the auxin polar transport activity in the *ifl1* mutant inflorescence stems should not be altered. Further analysis of the relationship between the IFL1 function and the auxin polar flow will help us to better understand the mechanisms underlying the positional control of fiber differentiation. It also will extend our knowledge of the roles that HD-ZIP proteins play in the specification of positional information.

HD-ZIP Proteins and Sclerenchyma Differentiation

We previously proposed that studies of fiber differentiation might provide insights into the mechanisms controlling tracheary element differentiation (Zhong et al., 1997). This is because fibers are considered to develop by activating the same mechanisms for secondary wall formation as are used for tracheary element formation. Our finding that IFL1, an HD-ZIP protein, regulates fiber differentiation raises an interesting question regarding whether the other group III HD-ZIP proteins might be involved in the control of tracheary element differentiation. Studies with Athb8, another member of group III HD-ZIP proteins, indicated that this might be the case. It has been shown that the *Athb8* gene is preferentially expressed in the procambial region (Baima et al., 1995), suggesting that Athb8 might be involved in the regulation of tracheary element formation or vascular differentiation in general. The tissue-level expression patterns of the other two members of the group III HD-ZIP proteins have not been analyzed. Further characterization of these HD-ZIP genes will most likely provide new insights into the mechanisms controlling plant cell differentiation.

IFL1 and Vascular Differentiation

It is intriguing that the *IFL1* gene is highly expressed in both the interfascicular and fascicular regions of the inflorescence stems. The expression of *IFL1* in the interfascicular regions correlates well with the role of IFL1 in the control of interfascicular fiber differentiation. But does IFL1 play any roles in vascular differentiation?

Although the *ifl1* mutation completely abolishes normal interfascicular fiber differentiation, it only has a partial effect on vascular differentiation. Noticeably, the numbers of xylary fibers and tracheary elements were reduced in the vascular bundles of both *ifl* mutants. The most obvious effect was observed in the vascular bundles at the basal parts of the stems, in which no xylary fibers were induced in either *ifl* mutant. In addition, in the *ifl1-2* mutant, no xylary fibers were formed in the vascular bundles throughout the stems (Figure 9). This indicates that IFL1 plays a role in the differentiation of tracheary elements and fibers in the vascular bundles of stems. It is likely that IFL1 might be involved in one of multiple pathways controlling the formation of tracheary elements and fibers in the vascular bundles. Thus, mutations in the *IFL1* gene only result in a partial effect on the differentiation of xylary fibers and tracheary elements. It will be interesting to identify other genes involved in the differentiation of xylary fibers and tracheary elements. As discussed above, one of the possible candidates is the *Athb8* gene, which shows preferential expression in procambial regions (Baima et al., 1995).

Because xylary fibers, extraxylary fibers, and tracheary elements all are induced along the paths of auxin polar flow, it is reasonable to predict that IFL1 might regulate genes involved in the control of auxin flow or genes involved in the transduction of hormonal signals in both fascicular and interfascicular regions. Mutation of the *IFL1* gene might affect auxin flow through or the auxin signal transduction in the

fascicular regions, thus leading to an alteration in the differentiation of both xylary fibers and vessel elements in vascular bundles. The possibility that IFL1 regulates genes involved in auxin polar flow is especially appealing considering the differential effect on xylem differentiation along the stems observed in the *ifl1* mutant. The *ifl1* mutation exhibited a much more dramatic effect on xylem differentiation in the lower parts of the stems than in the upper parts. The severe defect in xylem differentiation in the lower parts of the stems could be due to an insufficient flow of auxin, which is produced at the apex and in young leaves, toward the basal stems.

This possibility also could explain the differential activities that occurred in the interfascicular regions along the stems of the *ifl1* mutant. It was shown that some interfascicular cells other than the cells normally destined to become fibers were sclerified in the upper parts of the stems in the *ifl1* mutant, whereas this did not happen in the lower parts of the stems (Zhong et al., 1997). The lack of sclerification of interfascicular cells in the lower parts of the *ifl1* stems could be due to an insufficient auxin flow toward the basal parts of the stems. Such a phenomenon—a reduction in auxin polar flow that results in a local alteration in vascular differentiation—has been observed in the *pin-formed* (*pin1*) mutant, in which an auxin efflux carrier is defective (Gälweiler et al., 1998). It is important to determine whether IFL1 regulates the genes involved in the control of auxin flow or genes involved in the transduction of hormonal signals. It also will be interesting to identify the downstream genes regulated by IFL1 and examine whether they play any roles in the differentiation of interfascicular and/or fascicular fibers.

METHODS

Generation of CAPS Markers for Fine Mapping

MIUP24 bacterial artificial chromosome (BAC) DNA was purified from bacteria containing the MIUP24 clone. End sequences of the DNA fragments obtained from digestion of the MIUP24 BAC DNA with BamHI, EcoRI, or EcoRV were used to develop new cleaved amplified polymorphic sequence (CAPS) markers for fine mapping of the *ifl1* locus. Conditions for polymerase chain reactions (PCRs) and restriction enzyme digestions used for mapping were essentially the same as described by Konieczny and Ausubel (1993).

Complementation of the *ifl1* Mutant

Overlapping DNA fragments (10 to 14 kb) spanning the region between mup24RI-6A and mup24B2 markers were excised from the pBluescript KS+ vector (Stratagene, La Jolla, CA) and ligated into the binary vector pBI101. The new constructs were transformed into Agrobacterium strain GV3101 by electroporation. Agrobacteria containing the constructs were used to transform the *ifl1* plants by using the vacuum infiltration–mediated transformation procedure (Bechtold and Bouchez, 1994; Bent et al., 1994). Transgenic plants were selected by growing on Murashige and Skoog medium (Murashige and Skoog, 1962) containing 50 mg/L kanamycin. The location of interfascicular fibers in the inflorescence stems of transgenic plants was examined by sectioning and staining with toluidine blue.

Isolation of *IFL1* cDNAs

cDNAs synthesized from mRNAs isolated from *Arabidopsis thaliana* inflorescence stems were ligated into the cloning vector λZAPII (Stratagene) to generate an Arabidopsis stem cDNA library. The library was screened for *IFL1* cDNA with radiolabeled probes, as described by Sambrook et al. (1989). Positive clones were identified and converted into phagemids for sequencing.

Sequencing of *IFL1* Genomic DNA and cDNA

The *IFL1* gene and cDNAs were cloned into the pBluescript KS+ vector and sequenced with the rodamine-dye sequencing kit (PE Applied Biosystems, Foster City, CA). Sequencing reactions were analyzed in the ABI 310 sequence detection system (PE Applied Biosystems). Genomic DNA sequence was analyzed for putative genes with the Baylor College of Medicine gene finder program. Comparison of the *IFL1* genomic DNA and cDNA sequences with sequences in the public database was performed by using the BLAST network service from the National Center for Biotechnology Information (Bethesda, MD). After we cloned the *IFL1* gene, the MIUP24 BAC DNA in which the *IFL1* gene is located was sequenced by the Japanese Arabidopsis sequencing group (Web site: http://www.kazusa.or.jp/arabi). The *IFL1* cDNA sequence data reported here appear in the GenBank Nucleotide Sequence Database under the accession number AF188994.

Sequencing of the *ifl1* Mutant cDNA

mRNAs isolated from the *ifl1* stems were reverse-transcribed into cDNAs. The transcribed cDNAs then were used to PCR-amplify full-length *ifl* cDNAs with primers (5′-ATGGCGGTGGCTAACCACCGTGAG-3′ and 5′-TCACACAAAAGACCAGTTTACAAA-3′). The amplified *ifl1* and *ifl1-2* mutant cDNAs were sequenced as described above.

Transient Expression in Onion Epidermal Cells

The full-length *IFL1* cDNA without the stop codon was inserted in-frame in front of the β-glucuronidase (*GUS*) gene in the pBI121 vector. Similarly, DNA fragments encoding the homeodomain–leucine zipper (HD-ZIP) region or the C-terminal region of IFL1 with an added start codon were inserted in-frame in front of the *GUS* gene in pBI121. Expression of the fusion gene was driven by the cauliflower mosaic virus 35S promoter. Plasmid DNA coated onto 1-μm gold particles (BioRad, Hercules, CA) was introduced into onion epidermal cells with the Helium Biolistic gene transfomation system (Du Pont, Wilmington, DE), as described by Varagona et al. (1992). After particle bombardment, the onion peels were incubated on Murashige and Skoog medium (Murashige and Skoog, 1962) for 16 hr at room temperature. The GUS activity in the cells was detected as described (Jefferson et al., 1987) by incubating the onion peels in a staining solution (100 mM sodium phosphate, pH 7.0, 10 mM EDTA, 0.5 mM

ferricyanide, 0.5 mM ferrocyanide, and 1 mM 5-bromo-4-chloro-3-indolyl β-D-glucuronic acid) overnight at 37°C.

RNA Isolation and Gel Blot Analysis

Total RNA was isolated from Arabidopsis organs as described previously (Ye and Varner, 1993). Poly(A)$^+$ RNA used for cDNA synthesis was isolated using a Poly-A-Tract mRNA isolation system (Promega, Madison, WI), following the manufacturer's protocol. RNA gel blot analysis was performed as described previously (Ye and Varner, 1993).

In Situ Localization of the *IFL1* mRNA

Inflorescence stems of 6-week-old Arabidopsis plants were fixed, dehydrated, and embedded in paraffin. Thin sections were prepared from paraffin-embedded stems and used for *IFL1* mRNA localization as described previously (Jackson, 1991).

A 600-bp *IFL1* cDNA fragment was amplified by PCR with primers (5′-TGGAGCTTGTTCTGAACTGAT-3′ and 5′-CAAGTGTTGTCTCTAGCATGT-3′) and ligated into a pBluescript vector for making RNA probes. The pBluecript KS+ vector containing the *IFL1* cDNA fragment was used to make sense and antisense digoxigenin (DIG)-labeled *IFL1* RNA probes with a DIG RNA labeling system (Roche Molecular Systems, Branchburg, NJ). The DIG-labeled *IFL1* RNA probes were used in the hybridization reaction on Arabidopsis stem sections. The hybridization signals were detected by incubating with gold-conjugated antibodies against DIG. Bound gold particles were revealed by a silver enhancement kit (Amersham, Piscataway, NJ). Sections then were counterstained with 0.5% safranin-*O* to show anatomical structure.

Analysis of *IFL1* Promoter Activity in Transgenic Plants

A 2.3-kb genomic DNA fragment upstream of the *IFL1* transcribed sequence was PCR-amplified with primers (5′-GTCGAAGAGGTTTAGTCGTAT-3′ and 5′-CCGCCATCTCCATTTTAGCT-3′). The amplified *IFL1* promoter fragment was cloned into the pBluescript vector and sequenced to make sure that the PCR fragment had no point mutations due to PCR reactions. The *IFL1* promoter then was inserted into the polylinker region upstream of the GUS reporter sequence in the pBI101 vector. The construct was introduced into Agrobacterium strain GV3101 by electroporation. Agrobacteria containing the construct were used to transform Arabidopsis (ecotype Columbia) plants with the vaccum infiltration method (Bechtold and Bouchez, 1994; Bent et al., 1994), and transgenic plants were selected by growing on Murashige and Skoog medium (Murashige and Skoog, 1962) containing kanamycin. Leaves, roots, and segments of inflorescence stems of the transgenic plants were stained for GUS activity according to Jefferson et al. (1987) by incubation in a staining solution (100 mM sodium phosphate, pH 7.0, 10 mM EDTA, 0.5 mM ferricyanide, 0.5 mM ferrocyanide, and 1 mM 5-bromo-4-chloro-3-indolyl β-D-glucuronic acid) at 37°C. The tissues then were incubated in 100% ethanol to remove chlorophyll. The stained leaves and roots were observed directly under a dissection microscope. The stained stem segments were hand sectioned, and the sections were observed under a compound microscope.

ACKNOWLEDGMENTS

We thank Dr. Barbara Kunkle for providing Agrobacterium strain GV3101, and the Arabidopsis Biological Resource Center (Ohio State University, Columbus) for providing the YAC and BAC clones. This work was supported by the Cooperative State Research, Education, and Extention Service, U.S. Department of Agriculture.

Received August 17, 1999; accepted September 15, 1999.

REFERENCES

Affolter, M., Schier, A., and Gehring, W.J. (1990). Homeodomain proteins and the regulation of gene expression. Curr. Biol. **2,** 485–495.

Aloni, R. (1979). Role of auxin and gibberellin in differentiation of primary phloem fibers. Plant Physiol. **63,** 609–614.

Aloni, R. (1982). Role of cytokinin in differentiation of secondary xylem fibers. Plant Physiol. **70,** 1631–1633.

Aloni, R. (1987). Differentiation of vascular tissues. Annu. Rev. Plant Physiol. **38,** 179–204.

Aoyama, T., Dong, C.-H., Wu, Y., Carabelli, M., Sessa, G., Ruberti, I., Morelli, G., and Chua, N.-H. (1995). Ectopic expression of the *Arabidopsis* transcriptional activator Athb-1 alters leaf cell fate in tobacco. Plant Cell **7,** 1773–1785.

Baima, S., Nobili, F., Sessa, G., Lucchetti, S., Ruberti, I., and Morelli, G. (1995). The expression of the *Athb-8* homeobox gene is restricted to provascular cells in *Arabidopsis thaliana.* Development **12,** 4171–4182.

Bechtold, N., and Bouchez, D. (1994). *In planta Agrobacterium*-mediated transformation of adult *Arabidopsis thaliana* plants by vacuum infiltration. In Gene Transfer to Plants, I. Potrykus and G. Spangenberg, eds (Berlin: Springer-Verlag), pp. 19–23.

Bent, A.F., Kunkel, B.N., Dahlbeck, D., Brown, K.L., Schmidt, R., Giraudat, J., Leung, J., and Staskawicz, B.J. (1994). *RPS2* of *Arabidopsis thaliana*: A leucine-rich repeat class of plant disease resistance genes. Science **265,** 1856–1860.

Fukuda, H. (1996). Xylogenesis: Initiation, progression, and cell death. Annu. Rev. Plant Physiol. Plant Mol. Biol. **47,** 299–325.

Gälweiler, L., Guan, C., Müller, A., Wisman, E., Mendgen, K., Yephremov, A., and Palme, K. (1998). Regulation of polar auxin transport by AtPIN1 in Arabidopsis vascular tissue. Science **282,** 2226–2230.

Gehring, W.J., Muller, M., Affolter, M., Percival-Smith, A., Billeter, M., Qian, Y.Q., Otting, G., and Wutherich, K. (1990). The structure of the homeodomain and its functional implications. Trends Genet. **6,** 323–329.

Graba, Y., Aragnol, D., and Pradel, J. (1997). *Drosophila* Hox complex downstream targets and the function of homeotic genes. Bioessays **19,** 379–388.

Hardtke, C.S., and Berleth, T. (1998). The Arabidopsis gene *MONOPTEROS* encodes a transcription factor mediating embryo axis formation and vascular development. EMBO J. **17,** 1405–1411.

Jackson, D. (1991). In situ hybridization in plants. In Molecular Plant Pathology: A Practical Approach, D.J. Bowles, S.J. Gurr, and M.J. McPherson, eds (London: Oxford University Press), pp. 163–174.

Jefferson, R.A., Kavanagh, T.A., and Bevan, M.W. (1987). GUS fusions: β-Glucuronidase as a sensitive and versatile gene fusion marker in higher plants. EMBO J. **6,** 3901–3907.

Kerstetter, R.A., and Hake, S. (1997). Shoot meristem formation in vegetative development. Plant Cell **9,** 1001–1010.

Konieczny, A., and Ausubel, F.M. (1993). A procedure for mapping Arabidopsis mutations using co-dominant ecotype-specific PCR-based markers. Plant J. **4,** 403–410.

Larkin, J.C., Marks, M.D., Nadeau, J., and Sack, F. (1997). Epidermal cell fate and patterning in leaves. Plant Cell **9,** 1109–1120.

Lewin, B. (1990). Genes IV. (Oxford, UK: Oxford University Press).

Liu, Y.G., Mitsukawa, N., Vazquez-Tello, A., and Whittier, R.F. (1995). Generation of a high-quality P1 library of *Arabidopsis* suitable for chromosome walking. Plant J. **7,** 351–358.

Lu, P., Porat, R., Nadeau, J.A., and O'Neill, S.D. (1996). Identification of a meristem L1 layer-specific gene in Arabidopsis that is expressed during embryonic pattern formation and defines a new class of homeobox genes. Plant Cell **8,** 2155–2168.

Lyndon, R.F. (1990). Plant Development. (London: Unwin Hyman Ltd).

Masucci, J.D., Rerie, W.G., Foreman, D.R., Zhang, M., Galway, M.E., Marks, M.D., and Schiefelbein, J.W. (1996). The homeobox gene *GLABRA2* is required for position-dependent cell differentiation in the root epidermis of *Arabidopsis thaliana.* Development **122,** 1253–1260.

Meijer, A.H., Scarpella, E., van Dijk, E.L., Qin, L., Taal, A.J.C., Rueb, S., Harrington, S.E., McCouch, S.R., Schilperoort, R.A., and Hoge, J.H.C. (1997). Transcriptional repression by Oshox1, a novel homeodomain leucine zipper protein from rice. Plant J. **11,** 263–276.

Murashige, T., and Skoog, F. (1962). A revised medium for rapid growth and bioassay with tobacco tissue cultures. Physiol. Plant. **15,** 473–497.

Qian, Y.Q., Billeter, M., Otting, G., Muller, M., Gehring, W.J., and Wuthrich, K. (1989). The structure of the *Antennapedia* homeodomain determined by NMR spectroscopy in solution: Comparison with procaryotic repressors. Cell **59,** 573–580.

Reiser, L., Modrusan, Z., Margossian, L., Samach, A., Ohad, N., Haughn, G.W., and Fischer, R.L. (1995). The *BELL1* gene encodes a homeodomain protein involved in pattern formation in the Arabidopsis ovule primordium. Cell **83,** 735–742.

Rerie, W.G., Feldmann, K.A., and Marks, M.D. (1994). The *GLABRA2* gene encodes a homeo domain protein required for normal trichome development in Arabidopsis. Genes Dev. **8,** 1388–1399.

Ruberti, I., Sessa, G., Lucchetti, S., and Morelli, G. (1991). A novel class of plant proteins containing a homeodomain with a closely linked leucine zipper motif. EMBO J. **10,** 1787–1791.

Sambrook, J., Fritsch, E.F., and Maniatis, T. (1989). Molecular Cloning: A Laboratory Manual. (Cold Spring Harbor, NY: Cold Spring Harbor Laboratory Press).

Schena, M., and Davis, R.W. (1992). HD-Zip proteins: Members of an Arabidopsis homeodomain protein superfamily. Proc. Natl. Acad. Sci. USA **89,** 3894–3898.

Schena, M., and Davis, R.W. (1994). Structure of homeobox-leucine zipper genes suggests a model for the evolution of gene families. Proc. Natl. Acad. Sci. USA **91,** 8393–8397.

Schena, M., Lloyd, A.M., and Davis, R.W. (1993). The *HAT4* gene of Arabidopsis encodes a developmental regulator. Genes Dev. **7,** 367–379.

Schiefelbein, J.W., Masucci, J.D., and Wang, H. (1997). Building a root: The control of patterning and morphogenesis during root development. Plant Cell **9,** 1089–1098.

Schindler, U., Beckmann, H., and Cashmore, A.R. (1993). HAT3.1, a novel Arabidopsis homeodomain protein containing a conserved cysteine-rich region. Plant J. **4,** 137–150.

Schmidt, R., Love, K., West, J., Lenehan, Z., and Dean, C. (1997). Description of 31 YAC contigs spanning the majority of *Arabidopsis thaliana* chromosome 5. Plant J. **11,** 563–572.

Sessa, G., Morelli, G., and Ruberti, I. (1993). The Athb-1 and -2 HD-Zip domains homodimerize forming complexes of different DNA binding specificities. EMBO J. **12,** 3507–3517.

Sessa, G., Steindler, C., Morelli, G., and Ruberti, I. (1998). The Arabidopsis *Athb-8*, *-9* and *-14* genes are members of a small gene family coding for highly related HD-ZIP proteins. Plant Mol. Biol. **38,** 609–622.

Szymanski, D.B., and Marks, M.D. (1998). *GLABROUS1* overexpression and *TRIPTYCHON* alter the cell cycle and trichome cell fate in Arabidopsis. Plant Cell **10,** 2047–2062.

Varagona, M.J., Schmidt, R.J., and Raikhel, N.V. (1992). Nuclear localization signal(s) required for nuclear targeting of the maize regulatory protein Opaque-2. Plant Cell **4,** 1213–1227.

Vollbrecht, E., Veit, B., Sinha, N., and Hake, S. (1991). The developmental gene *Knotted-1* is a member of a maize homeobox gene family. Nature **350,** 241–243.

Ye, Z.-H., and Varner, J.E. (1993). Gene expression patterns associated with in vitro tracheary element formation in isolated single mesophyll cells of *Zinnia elegans.* Plant Physiol. **103,** 805–813.

Zhong, R., Jennifer, J.T., and Ye, Z.-H. (1997). Disruption of interfascicular fiber differentiation in an Arabidopsis mutant. Plant Cell **9,** 2159–2170.